J. Fluid Mech. (1968), *vol.* 34, *part* 1, *pp.* 49–80
Printed in Great Britain

Double Kelvin waves with continuous depth profiles

By M. S. LONGUET-HIGGINS
Oregon State University, Corvallis, Oregon

(Received 1 January 1968)

The possibility of long waves in a rotating ocean being trapped along a straight discontinuity in depth was demonstrated in a recent paper (Longuet-Higgins 1968). The analysis is now extended to the situation where the depth varies continuously, in a zone separating two regions of different depths. The trapping of waves in the transition zone is investigated, taking full account of the horizontal divergence of the motion.

If the profile of the depth is assumed to be monotonic, then it is shown that the trapped waves always travel along the transition zone with the shallower water to their right in the northern hemisphere and to their left in the southern hemisphere. The wave period must always exceed a pendulum-day. The period is also bounded below by a quantity depending inversely on the maximum bottom gradient.

By allowing the width W of the transition zone to vary, asymptotic forms for the trapped modes are obtained, both as $W \to 0$ and as $W \to \infty$. In the limit as $W \to 0$ the depth becomes discontinuous, and it is shown that the *lowest* mode then becomes a double Kelvin wave (Longuet-Higgins 1968) propagated along the discontinuity. The periods of the higher modes, on the other hand, all tend to infinity; these modes become steady currents.

Numerical calculations of the trapped modes are presented for two different laws of depth in the transition zone. It is found that as $W \to 0$ the lowest mode is insensitive to the form of the depth profile. Higher modes depend on the details of the profile. Hence the lowest mode is the most likely to be observed in the real ocean.

The dispersion relation is also investigated. It is shown that the group-velocity of all modes must change sign at some point in the range of wave-numbers, if the divergence is taken into account. When the divergence was neglected the lowest mode appeared to be exceptional, in that the group-velocity was always in the same direction. This anomaly is now removed.

1. Introduction

It was shown in a recent paper† that a discontinuity in depth in a rotating shallow sea is capable of supporting a novel kind of wave motion. The wave energy is propagated along the discontinuity, and falls off exponentially to either side. Such trapped waves have been called 'double Kelvin waves' or

† Longuet-Higgins (1968). This paper will subsequently be referred to as reference I.

'seascarp waves' (I). It was found that for any given wavelength, just one such wave motion is possible, and its period always exceeds one pendulum-day.

A discontinuity in the ocean depth is, however, a special and possibly uncommon situation. It is natural to inquire whether trapped waves exist when the bottom profile has other forms, for example, when there is a continuous transition from one depth to another. One may further ask whether such trapped waves will tend to double Kelvin waves as the width of the transition zone is reduced to zero.

An investigation of certain special cases has already been made both by Rhines (1967) and by Buchwald & Adams (1968). These authors, however, assumed that the divergence of the wave motion (associated with a vertical displacement of the free surface) was negligible. This assumption significantly affects the conclusions, as will be seen below. Rhines also made other approximations of a less significant nature (see footnote † on p. 53).

If the divergence is assumed to be negligible then it is not hard to see intuitively that waves will tend to be propagated along the sloping transition zone with the shallower water to their right, just as on a sloping plane bottom, or on a β-plane (see Longuet-Higgins 1965; §3; Phillips 1965). Those vertical filaments of fluid displaced up the slope are shortened and so have a negative relative velocity, and those displaced down the slope have a positive relative vorticity. The combination of alternate positive and negative vorticities results in a phase velocity to the west on a β-plane, or with shallow water to the right on a sloping bottom in the northern hemisphere. Outside the transition zone the above mechanism ceases to act, and one might therefore expect some types of wave in which the energy was mainly limited to the transition zone.

However, when the divergence is taken into account some stretching of the vertical filaments of water is caused also by the vertical displacement of the free surface, as well as by the bottom slope. At first sight it is not clear which of these effects will predominate.

In the present paper we take the divergence of the wave motion fully into account, and investigate the possibility of trapped wave motions being associated with continuous depth profiles of a rather general kind. The depth h is assumed to be a function only of the co-ordinate x normal to the escarpment. Moreover, h is assumed to be monotonic in x and to tend to uniform values at large distances from the escarpment on either side (see figure 1). The possibility of trapped waves in such a configuration is investigated on the basis of the linearized theory of waves in shallow water.

In §3 it is shown, first, that the waves can be propagated in one direction only, namely with the shallower water to the right of the direction of propagation. For sufficiently large wave periods, some trapped waves are always possible. Next, in §4 it is proved that the period τ must always exceed one pendulum-day. It is proved further that τ is bounded below by various bounds inversely proportional to the maximum slope of the bottom—the gentler the maximum bottom slope, the longer the wave period.

Next the asymptotic forms of the waves are found for very gentle slopes and very steep slopes, respectively. For very gentle slopes it is shown that with a symmetrical profile the energy tends to be located towards the upper part of the slope. There is a marked difference in asymptotic behaviour according as the bottom slope is smooth or discontinuous (as with a uniform slope connecting two different levels). On the other hand, for steep slopes it is found that there is one mode—the lowest, which tends to the double Kelvin wave as the width of the transition zone is diminished; and an infinity of higher modes whose periods each tend to infinity; these reduce to steady currents.

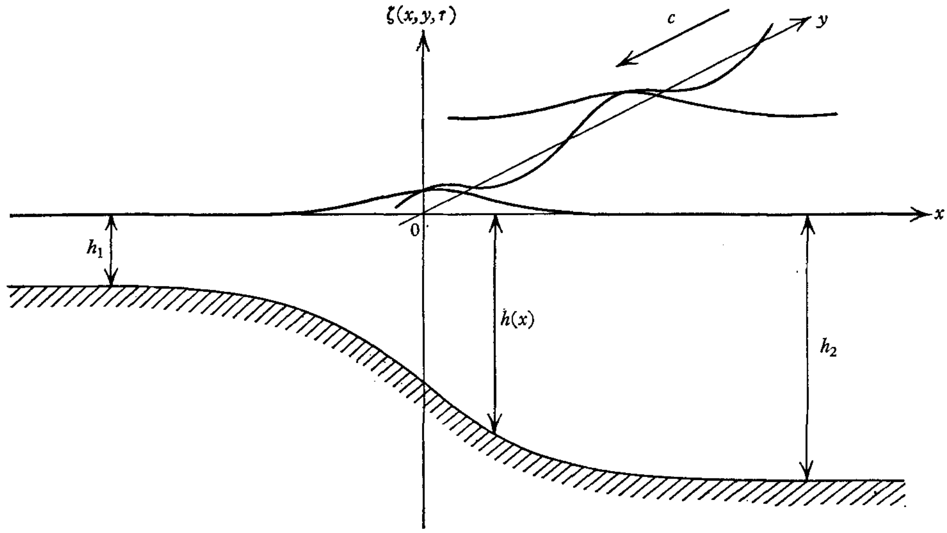

FIGURE 1. Trapped waves being propagated along the transition zone between two regions of uniform depth. The depth profile has the form given by equation (1.1).

In §§9 and 10 the asymptotic formulae are applied to the depth profile

$$h(x) = \bar{h}(1+\beta\tanh(x/W)) \tag{1.1}$$

which represents a smooth transition from a depth $\bar{h}(1-\beta)$ to a depth $\bar{h}(1+\beta)$; and secondly to the profile

$$h(x) = \begin{cases} \bar{h}(1-\beta) & (-\infty < x \leqslant -W), \\ \bar{h}(1+\beta x/W) & (-W \leqslant x \leqslant W), \\ \bar{h}(1+\beta) & (W \leqslant x < \infty) \end{cases} \tag{1.2}$$

which represents a zone of uniform gradient joining two regions of different but uniform depth. Numerical calculations of the wave period τ and some profiles of the trapped waves are presented for the whole range of widths of the transition zone.

In §11, we discuss the dispersion relation—connecting the frequency σ of the waves with the wave-number m parallel to the escarpment. It is shown that $\sigma \to 0$ both when $m \to 0$ and when $m \to \infty$, for all modes including the lowest, provided the divergence of the waves is taken into account. Hence the group velocity is always in the same direction as the phase velocity at small wave-numbers, and in the opposite direction at large wave-numbers. Some computations of the dispersion relation for the profile (1.1) are shown in figures 11 and 12.

The behaviour of the lowest mode, in which the frequency tends to zero as $m \to 0$ is in contrast to that found by Buchwald & Adams (1968) in the case when the depth profile $h(x)$ in the transition zone is exponential. They found that as $m \to 0$ the frequency tended to a non-zero value. We show in § 11 that this difference is due to their neglect of the horizontal divergence of the wave motion.

2. General equations

We take as our starting point the linearized equations of motion and the equation of continuity for long waves in a rotating plane:

$$\frac{\partial u}{\partial t} - fv = -g\frac{\partial \zeta}{\partial x}, \tag{2.1}$$

$$\frac{\partial v}{\partial t} + fu = -g\frac{\partial \zeta}{\partial y}, \tag{2.2}$$

$$\frac{\partial}{\partial x}(hu) + \frac{\partial}{\partial y}(hv) = -\frac{\partial \zeta}{\partial t}, \tag{2.3}$$

where x and y are horizontal rectangular co-ordinates, t denotes the time, u and v the velocity components in the x- and y-directions, ζ the surface elevation, and f, g and h the Coriolis parameter, the acceleration of gravity and the equilibrium depth respectively. h is in general a function of x and y.

Suppose now that h is independent of y, and let us seek solutions in the form of waves travelling in the y-direction (see figure 1). Thus let

$$u, v, \zeta \propto e^{i(my - \sigma t)}, \tag{2.4}$$

where σ denotes the radian frequency and m is the wave-number in the y-direction. Without loss of generality we may take $m > 0$. On replacing $\partial/\partial t$ by $(-i\sigma)$ and $\partial/\partial y$ by (im) in equations (2.1) and (2.2), and solving we obtain a pair of simultaneous equations for u and v whose solution is

$$\left.\begin{aligned} u &= \frac{ig}{f^2 - \sigma^2}\left(\sigma\frac{\partial}{dx} - fm\right)\zeta, \\ v &= \frac{g}{f^2 - \sigma^2}\left(f\frac{\partial}{dx} - \sigma m\right)\zeta. \end{aligned}\right\} \tag{2.5}$$

Substitution in (2.3) now gives the following equation for ζ

$$\frac{d}{dx}\left(h\frac{d\zeta}{dx}\right) = \left(\frac{f^2 - \sigma^2}{g} + m^2 h + \frac{mf}{\sigma}\frac{dh}{dx}\right)\zeta. \tag{2.6}$$

We shall assume that the bottom slope is monotonic, that is to say

$$dh/dx \geqslant 0. \tag{2.7}$$

(see figure 1). Also that as $x \to -\infty$ so $h \to h_1 > 0$; and that as $x \to +\infty$ so $h \to h_2 < \infty$. We then seek solutions to equation (2.6) in the form of 'trapped' modes—that is, solutions in which $\zeta \to 0$ as $x \to \pm\infty$.

It may be recalled (I) that when $\sigma^2 < f^2$ the parameter ϵ defined by

$$\epsilon = f^2/m^2gh_2 \tag{2.8}$$

is a measure of the divergence of the wave motion in deep water. In the non-divergent approximation used by Rhines (1967) and Buchwald & Adams (1968) it is assumed that $\epsilon \ll 1$, so that the first term on the right of (2.6) may be omitted. Here we shall not make this assumption.†

3. The form of the solutions

It is convenient to choose units of length and time in which

$$m = 1, \quad f = 1 \tag{3.1}$$

and to write

$$\tau = -f/\sigma = -1/\sigma \tag{3.2}$$

for the period in pendulum-days. We shall see shortly that τ is always positive. Equation (2.6) then assumes the form

$$\frac{d}{dx}\left(h\frac{d\zeta}{dx}\right) = \left(\frac{\tau^2-1}{g\tau^2} + h - \tau\frac{dh}{dx}\right)\zeta. \tag{3.3}$$

We look for eigensolutions of (3.3), that is for values of τ for which there is a solution (3.3) tending to 0 as $x \to \pm\infty$. We shall see that there is an infinite discrete sequence $\tau_0, \tau_1, \ldots$ of such eigenvalues.‡

The asymptotic behaviour of ζ as $x \to \pm\infty$ is simple; for since h tends monotonically to a constant, dh/dx must tend to 0. Thus at $x = -\infty$, for example, (3.3) becomes

$$h_1\frac{d^2\zeta}{dx^2} = \left(\frac{\tau^2-1}{g\tau^2} + h_1\right)\zeta. \tag{3.4}$$

The coefficient of ζ is a constant. Since $\zeta \to 0$ as $x \to -\infty$ we must have

$$\zeta \sim \text{constant} \times \exp(l_1 x) \tag{3.5}$$

where

$$l_1^2 = \frac{\tau^2-1}{gh_1} + 1 \quad (l_1 > 0). \tag{3.6}$$

Similarly as $x \to +\infty$ the solution is given asymptotically by

$$\zeta \sim \text{constant} \times \exp(l_2 x), \tag{3.7}$$

where

$$l_2^2 = \frac{\tau^2-1}{gh_2} + 1 \quad (l_2 < 0). \tag{3.8}$$

† In the corresponding equation for the stream function in non-divergent motion, Rhines also replaced the factor h on the left-hand side by a constant $\bar{h}$. Here we take the variation of h fully into account, as well as the divergence.

‡ The eigenvalue problem is not of the standard Sturm–Lionville form since τ occurs in a non-linear manner. It may perhaps be put into the form studied by Shinbrot (1963) but it is not clear that all of Shinbrot's conditions are satisfied.

Moreover, both l_1 and l_2 are real; hence

$$\frac{\tau^2-1}{g\tau^2}+h_1 > 0, \tag{3.9}$$

and similarly for h_2.

In general the behaviour of ζ is exponential or sinusoidal in character according as the coefficient of ζ in equation (3.3) is positive or negative, that is according to the sign of

$$Q = \frac{\tau^2-1}{g\tau^2}+h-\tau\frac{dh}{dx}. \tag{3.10}$$

If Q is positive throughout the whole range of x we see from (3.3) that ζ and $(hd\zeta/dx)$ must have the same sign not only when $x \to -\infty$ but throughout the

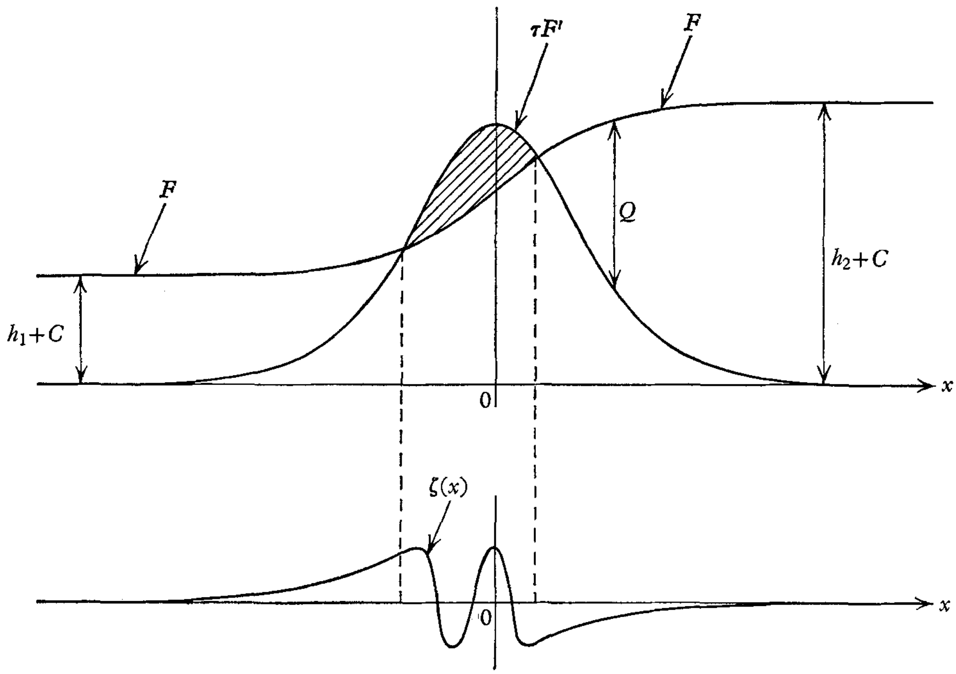

FIGURE 2. Sketch of the functions F, $\tau F'$ and Q defined by (3.14) and (3.15) when the depth profile is given by (1.1). Below is sketched one of the trapped modes ($n = 3$).

whole range of x. Hence ζ must tend to $\pm\infty$ as $x \to \infty$, and the solution cannot represent a trapped wave. So for a trapped wave to exist, Q must change sign somewhere in $(-\infty, \infty)$, that is

$$\tau\frac{dh}{dx} > \frac{\tau^2-1}{g\tau^2}+h \tag{3.11}$$

for at least some x in $(-\infty, \infty)$. Since $h \geqslant h_1$ this implies

$$\tau\frac{dh}{dx} > \frac{\tau^2-1}{g\tau^2}+h_1 > 0 \tag{3.12}$$

by (3.9). But m and dh/dx are both positive, by hypothesis; therefore we have

$$\tau > 0. \tag{3.13}$$

It follows that *in* the northern hemisphere, where $f > 0$, the trapped waves can be propagated only in the negative y-direction, that is to say with the shallower water to the right. In the southern hemisphere the shallower water is to the left of the direction of propagation.

Let us consider the function Q of equation (3.10). Q may be expressed as the difference of two terms:

$$Q = F - \tau F' \tag{3.14}$$

where

$$F = h + C, \qquad C = \frac{\tau^2 - 1}{g\tau^2} \tag{3.15}$$

and a prime denotes d/dx. The graph of F is the reflexion of the depth profile in the line parallel to the x-axis at a distance $\frac{1}{2}C$ (see figure 2). We have seen that F is always positive, The derivative F' is also positive or zero, by hypothesis, so that $\tau F'$ is a non-negative function of x.

Now for trapped waves to exist, the difference Q must be negative over some range of x (corresponding to the shaded area in figure 2). Within this 'potential well' the wave profile ζ is sinusoidal; outside, it is exponential. It can be seen from figure 2 that if the profile of the bottom is anti-symmetrical about $x = 0$, then the limits of the 'potential well' will be displaced somewhat to the left. So we expect the wave energy to be displaced towards the upper part of the slope.

Since increasing τ tends to increase both F and $\tau F'$, the effect on Q at moderate values of τ is not clear. However, as $\tau \to \infty$, so $F \to h + 1/g$, and so Q may be made as negative as we please wherever $F' > 0$. Hence we see that an infinite sequence of eigenvalues τ must exist, tending to infinity. We shall now establish some lower bounds for τ.

4. Bounds for the wave period

Using a prime to denote differentiation with respect to x, we may write (3.3) concisely as

$$(h\zeta')' = \left(\frac{\tau^2 - 1}{g\tau^2} + h - \tau h'\right)\zeta. \tag{4.1}$$

Let us multiply both sides of this equation by ζ' and integrate over $-\infty < x < \infty$:

$$\int (h\zeta')'\zeta'\,dx = \int \left(\frac{\tau^2 - 1}{g\tau^2} + h - \tau h'\right)\zeta\zeta'\,dx \tag{4.2}$$

(the limits of integration being understood). Because of the exponential behaviour of ζ at $\pm\infty$ the resulting integrals converge easily. The left-hand side, on integrating by parts, can be transformed as follows:

$$\int (h\zeta')'\zeta'\,dx = -\int h\zeta'\zeta''\,dx = \int h'\tfrac{1}{2}\zeta'^2\,dx. \tag{4.3}$$

Similarly, the right-hand side becomes

$$-\int (h' - \tau h'')\tfrac{1}{2}\zeta^2\,dx. \tag{4.4}$$

On equating the two sides one obtains, for τ, the relation

$$\tau \int h''\zeta^2 dx = \int h'(\zeta^2 + \zeta'^2)\, dx. \tag{4.5}$$

The integrand on the right is non-negative, and since we have seen that $\tau > 0$ it follows that

$$\int h''\zeta^2 dx > 0. \tag{4.6}$$

Let us now subtract from each side of (4.5) the corresponding side of the equation

$$\int h''\zeta^2 dx = -\int h' 2\zeta\zeta'\, dx. \tag{4.7}$$

We obtain
$$(\tau - 1)\int h''\zeta^2 dx = \int h'(\zeta + \zeta')^2 dx. \tag{4.8}$$

Since the integrand on the right is non-negative it follows (except in the trivial case $h' \equiv 0$) that the right-hand side is positive. But the integral on the left is also positive, by (4.6). We have therefore

$$(\tau - 1) > 0 \quad (\tau > 1). \tag{4.9}$$

In other words, the wave period necessarily exceeds one pendulum-day.

Now let us return to equation (4.1), multiply this time by ζ and integrate again over $(-\infty, \infty)$. After integrating the left-hand side by parts we obtain now

$$-\int h\zeta'^2 dx = \int \left(\frac{\tau^2 - 1}{g\tau^2} + h - \tau h'\right) \zeta^2 dx. \tag{4.10}$$

Since the left-hand side is negative, the integrand on the right must be negative over some range of x. Hence

$$\tau > 1 \Big/ \left(\frac{h'}{h}\right)_{\max} > \frac{h_1}{(h')_{\max}}. \tag{4.11}$$

In other words the period is bounded below not only by 1 but by a quantity inversely proportional to the maximum bottom slope. More strictly, (4.11) relates τ to the maximum proportional rate of change of depth.

In (4.10) let us take over to the left-hand side those terms involving τ explicitly:

$$\int \left(\tau h' - \frac{\tau^2 - 1}{g\tau^2}\right) \zeta^2 dx = \int h(\zeta^2 + \zeta'^2)\, dx. \tag{4.12}$$

Now adding to each side of this equation the corresponding side of the identity

$$-\int h'\zeta^2 dx = \int h 2\zeta\zeta'\, dx, \tag{4.13}$$

we obtain
$$(\tau - 1)\int \left(h' - \frac{\tau + 1}{g\tau^2}\right) \zeta^2 dx = \int h(\zeta + \zeta')^2 dx. \tag{4.14}$$

As before, the right-hand side is positive. Since also $(\tau - 1) > 0$ by (4.9) it follows that

$$\int \left(h' - \frac{\tau + 1}{g\tau^2}\right) \zeta^2 dx > 0. \tag{4.15}$$

Therefore the integrand must be positive over at least some range of x. Consequently

$$(h')_{\max} > \frac{\tau+1}{g\tau^2}, \tag{4.16}$$

that is

$$\tau^2(gh')_{\max} - \tau - 1 > 0. \tag{4.17}$$

The product of the two roots of the quadratic expression on the left of (4.17) is equal to $-1/(gh')_{\max}$. Since this is negative, it follows that if the roots are real, one root is positive and the other negative. But τ is certainly positive. Hence τ must exceed the positive root, that is

$$\tau > \frac{1}{2(gh')_{\max}}[1+\{1+4(gh')_{\max}\}^{\frac{1}{2}}]. \tag{4.18}$$

Since the square root is certainly greater than 1 we have *a fortiori*

$$\tau > \frac{1}{(gh')_{\max}}. \tag{4.19}$$

This inequality is stronger than (4.11) whenever

$$gh_1 < 1. \tag{4.20}$$

5. Effects of small variations in depth or wavelength

From the analysis of §4 we may further deduce how the wave period varies when small changes are made to the depth $h(x)$. Equation (4.12) (unlike (4.5)) yields a variational principle, that is to say for a given law of depth $h(x)$, the value of τ is stationary with respect to small departures $\Delta\zeta(x)$ of the surface elevation from a solution ζ to the differential equation (4.1). This is easily verified by substituting $(\zeta+\Delta\zeta)$ in place of ζ in equation (4.12) and integrating by parts. Hence when h undergoes a small variation Δh, any change $\Delta\tau$ in the wave period arises, to first order, solely from the change in h. In fact we have from (4.12),

$$\Delta\tau\int\left(h'-\frac{2}{g\tau^3}\right)\zeta^2 dx = \int \Delta h(\zeta^2+\zeta'^2)dx - \tau\int\Delta h'\zeta^2 dx \tag{5.1}$$

$$= \int\Delta h(\zeta+\zeta')^2 dx - (\tau-1)\int\Delta h'\zeta^2 dx \tag{5.2}$$

$$= \int\Delta h(\zeta^2+\zeta'^2+2\tau\zeta\zeta')dx. \tag{5.3}$$

(The equivalence of (5.1), (5.2) and (5.3) follows after integration by parts.) From the identity

$$\left(h'-\frac{2}{g\tau^3}\right) \equiv \left(h'-\frac{\tau+1}{g\tau^2}\right)+\frac{(\tau-1)(\tau+2)}{g\tau^3} \tag{5.4}$$

combined with (4.14) we see that

$$\int\left(h'-\frac{2}{g\tau^3}\right)\zeta^2 dx = \frac{1}{\tau-1}\int h(\zeta+\zeta')^2 dx + \frac{(\tau-1)(\tau+2)}{g\tau^3}\int\zeta^2 dx > 0. \tag{5.5}$$

This shows that the coefficient of $\Delta\tau$ in (5.1) is strictly positive. Hence the sign of $\Delta\tau$ is the same as that of the right-hand sides of (5.1), (5.2) or (5.3).

Suppose, for example, that the depth h is increased by a constant quantity, so

$$\Delta h = \text{constant}, \quad \Delta h' = 0. \tag{5.6}$$

Then (5.1) shows that $\Delta\tau$ is necessarily positive. This is in accordance with the view that when we increase the depth we relax a constraint (namely the rigidity of the layer of fluid between depths h and $h+\Delta h$); hence the period τ is increased.

An integral formula for the group-velocity may be found similarly. For if the wave-number m is inserted in (4.12) we have via (2.6)

$$\int \left(m\tau h' - \frac{\tau^2-1}{g\tau^2}\right)\zeta^2 dx = \int h(m^2\zeta^2+\zeta'^2)\,dx. \tag{5.7}$$

Differentiating with respect to m we get

$$\frac{d\tau}{dm}\int \left(mh' - \frac{2}{g\tau^3}\right)\zeta^2 dx = 2m\int h\zeta^2 dx - \tau\int h'\zeta^2 dx. \tag{5.8}$$

The integral on the left has been shown to be positive. Therefore, the group-velocity, given by

$$c_g = \frac{d\sigma}{dm} = \frac{1}{\tau^2}\frac{d\tau}{dm} \tag{5.9}$$

is positive or negative according as

$$\int h\zeta^2 dx \gtrless \frac{\tau}{2m}\int h'\zeta^2 dx. \tag{5.10}$$

6. Dependence on horizontal scale

It was shown in paper I that when the depth profile has a sudden discontinuity separating two regions of uniform depth, a trapped wave may exist near the discontinuity. This situation may be regarded as the limiting case of a smooth depth profile when the horizontal scale of the profile is made to shrink continuously to zero. (The scale in the y-direction is meanwhile kept constant.)

We shall now consider the effect of the horizontal scale in a general way by assuming that the depth h is a function of x/W, where W is a parameter proportional to the width of the transition zone. Thus as $W\to\infty$ the transition zone stretches out to infinity, and the maximum slope tends to zero. As $W\to 0$ the transition zone becomes narrow and within this zone the bottom slope becomes very steep.

Let us write then

$$h = h(\xi) \quad \text{where} \quad \xi = x/W \tag{6.1}$$

and W denotes a positive parameter. In terms of ξ, the differential equation to be satisfied by the surface elevation is now

$$W^{-2}(h\zeta')' = \left(\frac{\tau^2-1}{g\tau^2} + h - W^{-1}\tau h'\right)\zeta, \tag{6.2}$$

where a prime denotes differentiation with respect to ξ. We propose to investigate the behaviour of the eigenvalues τ of this equation, and of the corresponding eigenfunctions $\zeta(\xi)$, as W varies over the whole range $(0, \infty)$.

We shall begin by determining the asymptotic behaviour of ζ and τ near the two extremes of the range of W, namely as $W \to \infty$ and $W \to 0$ respectively.

7. Gentle slopes: asymptotic forms of ζ as $W \to \infty$

Equation (6.2) may conveniently be written in the form

$$(h\zeta')' = W^2(F - \lambda F')\zeta, \tag{7.1}$$

where

$$\lambda = \tau / W \tag{7.2}$$

and

$$F = h + \frac{1}{g}\left(1 - \frac{1}{\lambda^2 W^2}\right). \tag{7.3}$$

(Here F denotes the same function as in (3.15), but now $F' = dF/d\xi = W\,dF/dx$.)

Since the maximum bottom slope is proportional to W^{-1} it follows from the inequality (4.11) that as $W \to \infty$ so

$$\tau \geqslant O(W) \quad \text{and} \quad \lambda \geqslant O(1). \tag{7.4}$$

So from (5.5)

$$F = h + \frac{1}{g} + O(W^{-2}). \tag{7.5}$$

In other words, F is independent of W, to second order in W^{-1}.

To fix the ideas, let us assume first that the depth profile is smooth, as in figure 2. Since F is a non-negative function of ξ, it follows that when λ is sufficiently small (but still $O(1)$ in W) then on the right of equation (7.1) $(F - \lambda F')$ is positive for all ξ and no trapped wave is possible. As soon as λ is increased sufficiently to make $(F - \lambda F')$ negative at some point, a solution becomes possible. Write

$$F - \lambda F' = G(\xi, \lambda) \tag{7.6}$$

and let ξ_0 and λ_0 denote the values of ξ and λ for which G just vanishes. At this point, if h'' exists, we must have

$$G_0 = 0, \quad G_0' = 0, \tag{7.7}$$

then the first two terms of the Taylor series

$$G = G_0 + (\xi - \xi_0)G_0' + (\lambda - \lambda_0)\frac{\partial G_0}{\partial \lambda} + \tfrac{1}{2}(\xi - \xi_0)^2 G_0'' + \dots \tag{7.8}$$

are zero, and since $\partial G_0/\partial\lambda = -F' + O(W^{-2})$ we have in the neighbourhood of (ξ_0, λ_0)

$$(h\zeta')' = W^2[\tfrac{1}{2}(\xi - \xi_0)^2 G_0'' - (\lambda - \lambda_0)(F_0' + O(W^{-2})) + \dots]. \tag{7.9}$$

Now writing

$$\xi - \xi_0 = X / W^{\frac{1}{2}}$$

and

$$\lambda - \lambda_0 = L / W \tag{7.10}$$

and retaining only the terms of lowest order in W we obtain

$$W h_0 (d^2\zeta/dX^2) = W^2[\tfrac{1}{2}G_0'' X^2/W - LF_0'/W]\zeta, \tag{7.11}$$

that is

$$(d^2\zeta/dX^2) = [(G_0''/2h_0)X^2 - (LF_0'/h_0)]\zeta. \tag{7.12}$$

This is a form of the harmonic oscillator equation

$$d^2\zeta/d\eta^2 = (\eta^2-\mu)\zeta \tag{7.13}$$

(also known as Weber's equation) in which

$$\eta = \left(\frac{G_0''}{2h_0}\right)^{\frac{1}{4}} X, \qquad \mu = \frac{LF_0'}{(G_0''/2h_0)^{\frac{1}{2}}}. \tag{7.14}$$

The only solutions that are finite as $\eta \to \pm\infty$ are given by

$$\zeta = e^{-\frac{1}{2}\eta^2} H_\nu(\eta) \qquad (\mu = 2\nu+1), \tag{7.15}$$

where H_ν denotes the Hermite polynomial of degree ν. From (7.14) and (7.15) it follows that

$$L = (2\nu+1)\left[\frac{h_0 G_0''}{2F_0'^2}\right]^{\frac{1}{2}} \qquad (\nu = 0, 1, 2, \ldots). \tag{7.16}$$

From (7.10) we have

$$\lambda = \lambda_0 + L/W, \tag{7.17}$$

where λ_0 is given by (7.7), that is to say by

$$\left.\begin{aligned} F_0 - \lambda F_0' &= 0,\\ F_0' - \lambda F_0'' &= 0. \end{aligned}\right\} \tag{7.18}$$

So we have to solve for ξ the equation

$$F_0 F_0'' - F_0'^2 = 0, \tag{7.19}$$

or

$$(\log F_0)'' = 0. \tag{7.20}$$

Then λ_0 is given by

$$\lambda_0 = F_0/F_0' = F_0'/F_0''. \tag{7.21}$$

Also

$$G_0'' = F_0'' - \lambda_0 F_0''' = \frac{F_0' F_0'' - F_0 F_0'''}{F_0'}. \tag{7.22}$$

Combining these results with (7.16) and (7.17) we have

$$\tau = \lambda W \sim \frac{F_0}{F_0'} W + (2\nu+1)\left[\frac{h_0(F_0'F_0'' - F_0 F_0''')}{2F_0'^3}\right]^{\frac{1}{2}}. \tag{7.23}$$

To the degree of approximation implied in (7.23), it is sufficient in solving (7.20) to take

$$F \sim h + (1/g) \tag{7.24}$$

(by (7.5)).

Thus we have obtained in general a discrete set of asymptotic solutions representing trapped waves. The eigenfunctions, given by (7.13), are in the form of Weber functions. The corresponding periods are given by (7.23). The wave profile has 0, 1, 2... zeros in $-\infty < \xi < \infty$, corresponding to the value of ν. Because of the exponential factor in (7.13) the energy is limited to the neighbourhood of the point $\xi = \xi_0$, surrounded by the small 'potential well'.

In §9 the above formulae will be applied to the smooth depth profile given by equation (1.1).

When, contrary to our hypothesis, h'' does not exist at the point ξ_0, then neither do F_0'' or G_0'. A slightly different asymptotic behaviour then occurs. One example of such a situation is the uniform-slope profile (1.2) (see figure 3). A sketch of the function Q is shown in figure 4. In such a situation the 'potential well' has a characteristic saw-toothed shape, with a discontinuity at the left-hand end ($\xi = \xi_0$). Within the potential well G has approximately the form

$$G = G_0 + (\xi - \xi_0) G'_{0+} + (\lambda - \lambda_0) \frac{\partial G_{0+}}{\partial \lambda}, \tag{7.25}$$

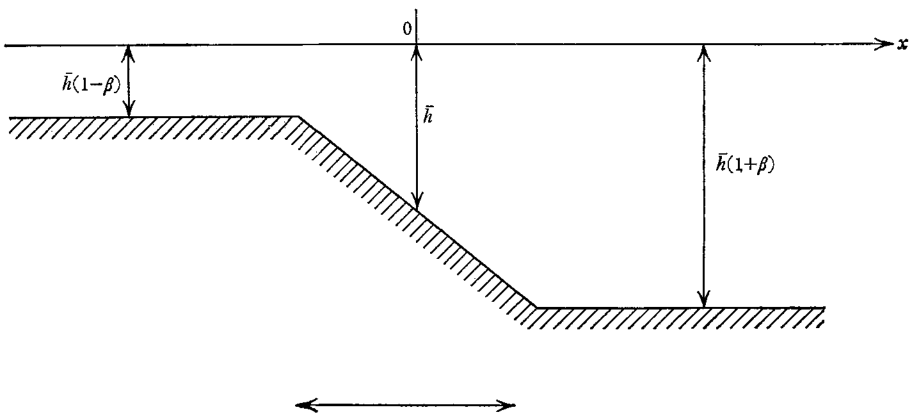

FIGURE 3. The form of the depth profile is given by equation (1.2).

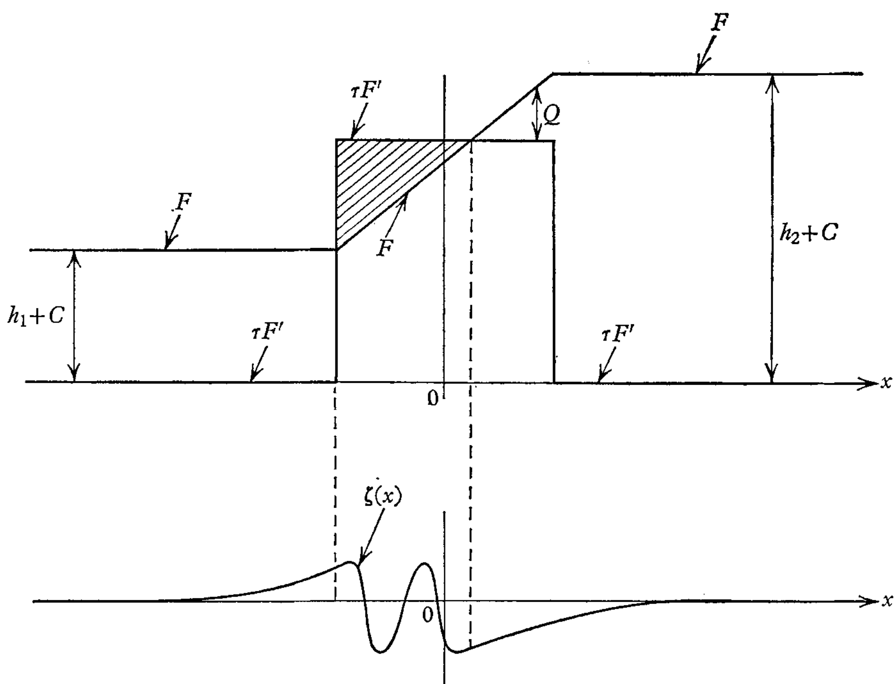

FIGURE 4. The form of the functions F, $\tau F'$ and Q for the depth profile (1.2). The fourth mode ($n = 3$) is sketched below.

where now G_0 vanishes and G'_{0+} represents the derivative of G to the right of $\xi = \xi_0$. Hence (7.1) becomes

$$(h\zeta')' = W^2[(\xi-\xi_0)G'_{0+} - (\lambda-\lambda_0)(F'_{0+}+O(W^{-2}))+\dots]\zeta \tag{7.26}$$

in contrast to equation (7.9). Now writing

$$\left.\begin{aligned} \xi-\xi_0 &= X/W^{\frac{2}{3}}, \\ \lambda-\lambda_0 &= L/W^{\frac{2}{3}} \end{aligned}\right\} \tag{7.27}$$

and retaining only the terms of lowest order, we obtain in place of (7.12) the equation

$$\frac{d^2\zeta}{dX^2} = [(G'_{0+}/h_0)X - (LF'_0/h_0)]\zeta. \tag{7.28}$$

The solution of this equation which vanishes as $x \to +\infty$ is given by

$$\zeta = Ai(\eta), \tag{7.29}$$

where

$$\eta = (G'_{0+}/h_0)^{\frac{1}{3}}(X - LF'_0/G'_{0+}) \tag{7.30}$$

and $Ai(\eta)$ denotes the Airy function.† As boundary condition at the left-hand end of the interval ($X = 0$) we note that ζ and $d\zeta/d\xi$ must both be continuous at $X = 0$. But to the left of the discontinuity $G(\xi)$ is of order 1 and so

$$d^2\zeta/d\xi^2 = O(W^2)\zeta.$$

Hence

$$d\zeta/d\xi = O(W)\zeta. \tag{7.31}$$

The same condition must hold to the right of the discontinuity. Hence

$$d\zeta/d\eta = O(W^{-\frac{2}{3}})d\zeta/d\xi = O(W^{-\frac{1}{3}})\zeta. \tag{7.32}$$

For large values of W this implies that the correct boundary condition, to lowest order in W^{-1}, is that ζ vanish when $X = 0$, that is

$$Ai(\eta) = 0 \quad \text{where} \quad \eta = -\frac{LF'_{0+}}{(h_0 G'^2_{0+})^{\frac{1}{3}}}. \tag{7.33}$$

Thus if the zeros of $Ai(\eta)$ are denoted by η_ν, where $\nu = 0, 1, 2, 3, \dots$ we have

$$L = -\frac{\eta_\nu (h_0 G'^2_{0+})^{\frac{1}{3}}}{F'_{0+}} \qquad (\nu = 0, 1, 2, \dots). \tag{7.34}$$

By (7.2) and (7.27) we have

$$\tau = \lambda W = \lambda_0 W + LW^{\frac{1}{3}}. \tag{7.35}$$

Since

$$\lambda_0 = F_0/F'_{0+} \tag{7.36}$$

and

$$G'_{0+} = F'_{0+} - \lambda_0 F''_{0+} = \frac{F'^2_{0+} - F_0 F''_{0+}}{F'_{0+}}, \tag{7.37}$$

we have

$$\tau \sim \frac{F_0}{F'_{0+}} W - \eta_\nu \left[\frac{h_0(F'^2_{0+} - F_0 F''_{0+})}{F'^4_{0+}}\right]^{\frac{1}{3}} W^{\frac{1}{3}}. \tag{7.38}$$

These formulae will be applied to the case of uniform slope in § 10.

† For tables of the Airy function and its zeros see Miller (1946) or Antosiewicz (1964).

8. Steep slopes; asymptotic forms as $W \to 0$

We now turn to the opposite end of the range of W, when the width W of the transition zone tends to zero.

Let the differential equation (6.2) be written in the form

$$(h\zeta')' = (W^2F - \bar{\lambda}F')\zeta, \tag{8.1}$$

where now

$$\bar{\lambda} = W\tau \tag{8.2}$$

and

$$F = h + (1/g)(1 - W^2/\bar{\lambda}^2). \tag{8.3}$$

We first seek solutions to (8.1) such that $\bar{\lambda} \geqslant O(1)$ as $W \to 0$.

As $W \to 0$ the first term W^2F on the right-hand side of (8.1) will become small compared to the second term $\bar{\lambda}F'$ whenever $F' > 0$. But since $F' \to 0$ when $\xi \to \pm\infty$ there will, for any W, always be points ξ_1 and ξ_2, say, where the two terms are in balance, i.e. where

$$W^2F - \bar{\lambda}F' = 0. \tag{8.4}$$

These may be called the turning points of the equation. If F' is strictly positive everywhere, as in the profile (1.1) then ξ_1 and ξ_2 tend to $\pm\infty$ respectively as $W \to 0$. Near or beyond the turning points, while ζ is $O(1)$, ζ' will tend to zero as $W \to 0$. Hence the asymptotic form of ζ will be that solution of the equation

$$(h\zeta')' + \bar{\lambda}F'\zeta = 0, \tag{8.5}$$

which satisfies the boundary conditions

$$\zeta' \to 0 \quad \text{as} \quad \xi \to \pm\infty. \tag{8.6}$$

An example of this will be given in §9.

If on the other hand F' vanishes identically outside a certain finite range (with the profile (1.2), this range is $(-1, 1)$), then ξ_1 and ξ_2 will tend respectively to the end-points of the range. The appropriate boundary conditions will be that

$$\zeta' = 0 \quad \text{as} \quad \xi \to \xi_1 \quad \text{or} \quad \xi_2. \tag{8.7}$$

An example will be given in §10.

It should be emphasized that $\zeta(\xi)$ will not necessarily tend to its asymptotic forms uniformly over the whole range of ξ. Such non-uniformity of convergence is a well-known characteristic of differential equations possessing turning points (see, for example, Olver 1955).

Both situations (8.6) and (8.7) lead generally to a well-posed eigenvalue problem having solutions $\zeta_n(\xi)$ and eigenvalues $\bar{\lambda}_n$, where

$$0 \leqslant \bar{\lambda}_0 < \bar{\lambda}_1 < \bar{\lambda}_2 < \dots. \tag{8.8}$$

Provided $\bar{\lambda}_n > 0$ it follows from (8.2) that as $W \to 0$

$$\tau_n \sim \bar{\lambda}_n/W \qquad (n = 1, 2, 3, \dots). \tag{8.9}$$

Thus the periods of these motions become infinite as the width W of the transition zone tends to zero. These motions reduce to steady currents.

However, one of the solutions of the limiting equation (8.5) is given by $\bar{\lambda} = \bar{\lambda}_0 = 0$ and $\zeta = \zeta_0 =$ constant. This solution contravenes our assumption that $\bar{\lambda} \geqslant O(1)$. But we already know from reference I that in the limiting case of discontinuous depth a solution does exist with finite τ, implying $\bar{\lambda} \to 0$ as $W \to 0$. Let us then re-investigate equation (8.1) on the assumption that $\tau \to \tau_0 > 0$. We shall calculate both the limiting value of τ and the next term in the expansion of τ in powers of W.

We return to equation (6.2) in the form

$$(h\zeta')' = \left[W^2\left(\frac{\tau^2-1}{g\tau^2}+h\right)-\frac{\tau}{\alpha}h'\right]\zeta. \tag{8.10}$$

Now for any finite value of W we have $h' \to 0$ as $\xi \to \pm\infty$. Hence as in §3 we have

$$\zeta \sim A\exp(Wl_1\xi) \quad \text{or} \quad B\exp(Wl_2\xi), \tag{8.11}$$

where A and B are constants and l_1 and l_2 are given by (3.6) and (3.8). Eliminating A and B we have the boundary conditions:

$$\left.\begin{aligned}\zeta' &\sim Wl_1\zeta \quad \text{as} \quad \xi \to -\infty,\\ \zeta' &\sim Wl_2\zeta \quad \text{as} \quad \xi \to +\infty.\end{aligned}\right\} \tag{8.12}$$

Suppose then that as $W \to 0$ and $W\xi \to \pm\infty$

$$\zeta \sim (1+O(W))\exp(Wl_j\xi) \quad (j = 1, 2) \tag{8.13}$$

and that as $W \to 0$ for fixed ξ

$$\zeta \sim 1+W\Delta\zeta. \tag{8.14}$$

Substituting from (8.14) into (8.10) and considering only the terms of lowest order in W we obtain

$$(h\Delta\zeta')' = -\tau h' \tag{8.15}$$

and from (8.12)

$$\left.\begin{aligned}\Delta\zeta' &\sim l_1 \quad \text{as} \quad \xi \to -\infty,\\ \Delta\zeta' &\sim l_2 \quad \text{as} \quad \xi \to +\infty,\end{aligned}\right\} \tag{8.16}$$

where l_1, l_2 and τ are the limiting values of these parameters as $W \to 0$. On integrating (8.15) we have

$$h\Delta\zeta' = -\tau h + A, \tag{8.17}$$

where A is a constant. But from (8.16)

$$A = h_1(l_1+\tau) = h_2(l_2+\tau). \tag{8.18}$$

Hence

$$\tau(h_2-h_1) = l_1h_1-l_2h_2. \tag{8.19}$$

This relation, together with the two relations (3.6) and (3.8), suffice to determine a unique set of finite, limiting values for the three unknowns l_1, l_2 and τ (see paper I). In fact τ is given by

$$\tau = (1-q^2)^{-\frac{1}{2}}, \tag{8.20}$$

where q is a root of the cubic equation

$$\omega q^3-(\omega-\alpha)q-1 = 0 \tag{8.21}$$

in which

$$\alpha = \frac{1}{2}\left[\left(\frac{h_2}{h_1}\right)^{\frac{1}{2}}+\left(\frac{h_1}{h_2}\right)^{\frac{1}{2}}\right], \quad \omega = \frac{1}{2g(h_1h_2)^{\frac{1}{2}}} = \frac{\epsilon}{2}\left(\frac{h_2}{h_1}\right)^{\frac{1}{2}}, \tag{8.22}$$

(see paper I, appendix). For example, when $h_2/h_1 = 2$ and $\epsilon = 1$ we find

$$\tau = 4{\cdot}496{,}48; \qquad l_1 = 1{\cdot}703{,}26; \qquad l_2 = -1{\cdot}396{,}62, \tag{8.23}$$

and in the special case $\epsilon = 0$ (non-divergent waves) we have, for all ratios h_2/h_1,

$$\tau = \frac{h_2+h_1}{h_2-h_1}; \qquad l_1 = 1; \qquad l_2 = -1 \tag{8.24}$$

in agreement with Rhines (1967).

Thus we have found a solution which, at least for finite values of ξ, tends to the solution for discontinuous depth. Various properties of this type of motion have been discussed in paper I. To a first approximation we have simply

$$\zeta = \begin{Bmatrix} \exp(Wl_1\xi) & (\xi < 0) \\ \exp(Wl_2\xi) & (\xi > 0) \end{Bmatrix} \tag{8.25}$$

so that the wave profile consists simply of two exponential curves back-to-back.

In the next approximation, when ξ is finite, the wave profile ζ is given by (8.14), where from (8.17)

$$\Delta\zeta' = -\tau + A/h \tag{8.26}$$

and so

$$\Delta\zeta = \int(-\tau + A/h)\,d\xi + \text{constant}. \tag{8.27}$$

From these results we can also calculate directly the rate of change of τ as the width W of the transition zone is increased from zero. For from the differential equation (6.2) it is straightforward to derive, as in (4.12), the variational principle

$$\int\left(\frac{\tau h'}{W} - \frac{\tau^2-1}{g\tau^2}\right)\zeta^2 d\xi = \int h(\zeta^2 + \zeta'^2/W^2)\,d\xi. \tag{8.28}$$

The value of τ is stationary with respect to arbitrary small perturbations of ζ. So on multiplying each side by W and differentiating with respect to W we find

$$\int\left(h' - \frac{2W}{g\tau^3}\right)\zeta^2 d\xi\left(\frac{d\tau}{dW}\right)_0 = \int\left[\left(h + \frac{\tau^2-1}{g\tau^2}\right)\zeta^2 - h\zeta'^2/W^2\right]d\xi. \tag{8.29}$$

In the integral on the left, we may use for ζ the first approximation (8.25), but on the right

$$\zeta'/W = \Delta\zeta' = A/h - \tau \tag{8.30}$$

by (8.25). Altogether we obtain

$$\left[(h_2-h_1) - \frac{1}{g\tau^3}\left(\frac{1}{l_2} - \frac{1}{l_1}\right)\right]\left(\frac{d\tau}{dW}\right)_0 = \int_{-\infty}^{\infty}\left[\left(h + \frac{\tau^2-1}{g\tau^2}\right) - h\left(\frac{A}{h} - \tau\right)^2\right]d\xi. \tag{8.31}$$

The integrand on the right-hand side tends to zero when $\xi \to \pm\infty$, and we assume that the integral converges. It is remarkable that only the right-hand side of this equation depends on the form of the function $h(\xi)$ in the transition zone.

Both the profiles (1.1) and (1.2) are anti-symmetrical with respect to ξ; and in this case the right-hand side takes a simpler form. Let us write it first as

$$\lim_{X\to\infty}\int_{-X}^{X}\left[\left(h+\frac{\tau^2-1}{g\tau^2}\right)-\left(\frac{A^2}{h}+2A\tau+\tau^2h\right)\right]d\xi$$
$$=\lim_{X\to\infty}\left\{2X\left[\left(\bar{h}+\frac{\tau^2-1}{g\tau^2}\right)-\left(\frac{A^2}{2h_1}+\frac{A^2}{2h_2}+2A\tau+\tau^2\bar{h}\right)\right]\right.$$
$$\left.-A^2\left[\int_{-X}^{0}\left(\frac{1}{h}-\frac{1}{h_1}\right)d\xi+\int_{0}^{X}\left(\frac{1}{h}-\frac{1}{h_2}\right)d\xi\right]\right\}. \quad (8.32)$$

Now the limit of the whole expression is independent of X. Therefore if the integrals each converge the coefficient of X must vanish. Hence we have simply

$$\left[(h_2-h_1)-\frac{1}{g\tau^3}\left(\frac{1}{l_2}-\frac{1}{l_1}\right)\right]\frac{\bar{h}}{A^2}\left(\frac{d\tau}{dW}\right)_0=\lim_{X\to\infty}\left[\left(\frac{X}{h_1}+\frac{X}{h_2}\right)-\int_{-X}^{X}\frac{d\xi}{h}\right]\bar{h}. \quad (8.33)$$

The right-hand side is now easily evaluated (see §§9 and 10). With $(d\tau/dW)_0$ given by this expression, we have as $W\to 0$

$$\tau\sim\tau_0+(d\tau/dW)_0W \quad (8.34)$$

9. The depth profile $h=\bar{h}\,(1+\beta\tanh x/W)$

We shall now determine the spectrum of trapped waves for the smooth bottom profile given by equation (1.1), that is to say

$$h/\bar{h}=1+\beta\tanh\xi. \quad (9.1)$$

First, let us apply the results of §§7 and 8.

(i) Asymptotic behaviour as $W\to\infty$

From (7.24) we have
$$F\sim\bar{h}\beta(\epsilon'+\tanh\xi), \quad (9.2)$$

where
$$\epsilon'=\frac{1}{\beta}\left(1+\frac{1}{g\bar{h}}\right)=\frac{1}{\beta}(1+\epsilon(1+\beta)). \quad (9.3)$$

Writing
$$\tanh\xi=\mu \quad (9.4)$$

we find
$$\left.\begin{aligned}F&\sim\bar{h}\beta(\epsilon'+\mu),\\F'&\sim\bar{h}\beta(1-\mu^2),\\F''&\sim\bar{h}\beta(-2\mu)(1-\mu^2).\end{aligned}\right\} \quad (9.5)$$

Equation (7.19) then reduces to

$$\mu_0^2+2\epsilon'\mu_0+1=0 \quad (9.6)$$

so that μ_0 (which is the root less than unity in absolute magnitude) is given by

$$\mu_0=-\epsilon'+(\epsilon'^2-1)^{\frac{1}{2}}. \quad (9.7)$$

Also
$$\lambda_0=F_0'/F_0''=-1/2\mu_0 \quad (9.8)$$

and, after some reduction,

$$\frac{h_0(F_0'F_0''-F_0F_0''')}{2F_0'^3} = \frac{1+\beta\mu_0}{-2\beta\mu_0}. \tag{9.9}$$

Hence as $W \to \infty$ we have

$$\tau \sim -\frac{1}{2\mu_0}W+(2\nu+1)\left(\frac{1+\beta\mu_0}{-2\beta\mu_0}\right)^{\frac{1}{2}} \qquad (\nu = 0,1,2,3,\ldots). \tag{9.10}$$

It will be seen from (9.7) that t_0 is negative, so that the central point of the 'potential well' lies somewhat to the left of the mid-point of the slope profile, as predicted. The eigenfunctions corresponding to (9.10) are given by

$$\zeta \sim e^{-\frac{1}{2}\eta^2}H_\nu(\eta) \tag{9.11}$$

where from (7.10) and (7.14)

$$\eta = \left(\frac{2\beta(1+\epsilon'\mu_0)^2}{1+\beta\mu_0}\right)^{\frac{1}{4}} W^{\frac{1}{2}}(\xi-\xi_0). \tag{9.12}$$

For example, when $\beta = \frac{1}{3}$ and $\epsilon = 1/gh_2 = 1$ we have

$$\epsilon' = 7, \qquad \mu_0 = 4\sqrt{(3)}-1, \qquad \xi_0 = -0{\cdot}071{,}920, \tag{9.13}$$

and

$$\tau \sim 6{\cdot}9641\,W+(2\nu+1)\times 4{\cdot}5158. \tag{9.14}$$

The asymptotes (9.14) are represented by the dashed curves on the right-hand side of figure 5. However, the asymptote corresponding to the lowest mode ($\nu = 0$) is so close to the exact value (found by numerical integration; see below) that it cannot be distinguished graphically. The reason for this will shortly become clear.

(ii) Asymptotic behaviour as $W \to 0$

On substitution from (9.1) the asymptotic equation (8.5) becomes

$$\frac{d}{d\xi}\left[\left(1+\beta\tanh\xi\right)\frac{d\zeta}{d\xi}\right]+L\,\mathrm{sech}^2\,\xi.\zeta = 0, \tag{9.15}$$

with

$$\frac{d\zeta}{d\xi}\to 0 \quad \text{as} \quad \xi\to\pm\infty. \tag{9.16}$$

In (9.15),

$$L = \beta\overline{\lambda} = \beta W\tau. \tag{9.17}$$

A change of variable to

$$\mu = \tanh\xi \tag{9.18}$$

reduces the problem to the solution of

$$\frac{d}{d\mu}\left[(1+\beta\mu)(1-\mu^2)\frac{d\zeta}{d\mu}\right]+L\zeta = 0 \tag{9.19}$$

subject to the condition that $d\zeta/d\mu$ be finite as $\mu\to\pm 1$. Equation (9.19) is a generalization of Legendre's differential equation, to which it reduces when $\beta = 0$. The solution is then given by

$$\zeta_0 = P_n(\mu), \quad L_0 = n(n+1) \quad (n = 1,2,3,\ldots). \tag{9.20}$$

In our application we must have $0 < \beta < 1$. The solutions to (9.19) are not known functions, but we may expand ζ and L in ascending powers of β as follows:

$$\left.\begin{aligned}\zeta &= \zeta_0+\beta\zeta_1+\beta^2\zeta_2+\ldots,\\ L &= L_0+\beta L_1+\beta^2L_2+\ldots,\end{aligned}\right\} \tag{9.21}$$

where ζ_0 and L_0 are given by (9.20). On substituting in (9.19) and using the relations

$$\left.\begin{aligned} (1-\mu^2)\frac{dP_n}{d\mu} &= \frac{n(n+1)}{2n+1}(P_{n-1}-P_{n+1}), \\ \mu P_n &= \frac{1}{2n+1}\{nP_{n-1}+(n+1)P_{n+1}\} \end{aligned}\right\} \tag{9.22}$$

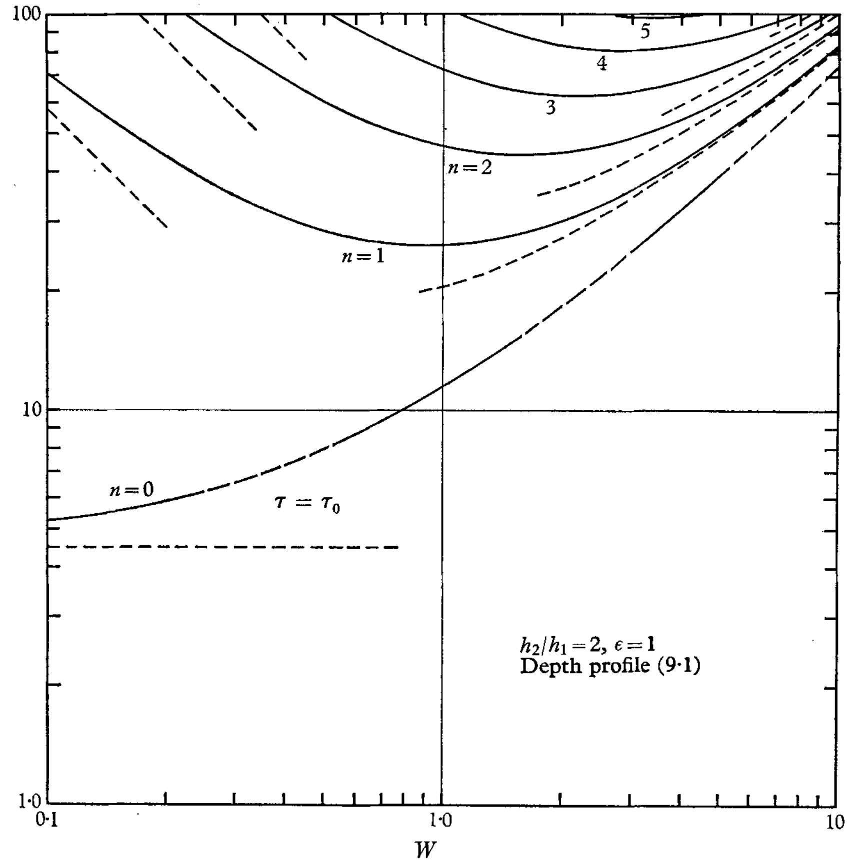

FIGURE 5. The period of the waves (in pendulum-days) as a function of the width W of the transition zone (multiplied by the wave-number m) when the depth profile has the form (9.1), with $\beta = \frac{1}{3}$, $\epsilon = 1$. Full curves represent the computed values. Broken curves represent asymptotes. For the lowest mode the curve cannot be distinguished from its asymptotes graphically.

we easily find $\zeta_1, \zeta_2, \ldots$ and $L_1, L_2, \ldots$ in succession. The first two terms in the series for ζ are found to be:

$$\left.\begin{aligned} \zeta_1 &= \frac{n^2-1}{4n+2}P_{n-1} - \frac{n(n+2)}{4n+2}P_{n+1}, \\ \zeta_2 &= \frac{(n-2)(n-1)^2 n(n+1)}{4(2n-1)^2(2n+1)}P_{n-2} + \frac{n(n+1)(n+2)^2(n+3)}{4(2n+1)(2n+3)^2}P_{n+2}. \end{aligned}\right\} \tag{9.23}$$

It is easy to show that L is an even function of β, so that the odd coefficients $L_1, L_3, \ldots$ all vanish. After some reduction we find

$$\left.\begin{aligned} \frac{L_2}{L_0} &= -\frac{3}{8}\left(1-\frac{1}{4m+1}\right), \\ \frac{L_4}{L_0} &= -\frac{3}{32}\left[1-\frac{9(m+1)+9m^2(4m-11)-m(m-1)(4m-11)}{(4m+1)^3\,(4m-11)}\right], \end{aligned}\right\} \tag{9.24}$$

where
$$m = n^2+n-1. \tag{9.25}$$

From (9.17) and (9.21) we have then

$$\tau_n \sim \frac{n(n+1)}{\beta}\left[1+\frac{L_2}{L_0}\beta^2+\frac{L_4}{L_0}\beta^4+\ldots\right]W^{-1}. \tag{9.26}$$

These asymptotic expressions are indicated in figure 5, by broken lines. The coefficients of W^{-1} are given in table 1 for $n = 1, 2, 3, 4, 5$.

n	$\bar{\lambda}_n$	
	Profile (1.1)	Profile (1.2)
1	5·79	7·25
2	17·26	28·83
3	34·49	64·78
4	57·46	115·11
5	86·17	179·83

Table 1. Coefficients of W^{-1} in the asymptotic expressions (9.26) and (10.18), when $\beta = \frac{1}{3}$

As pointed out in § 8, the case $n = 0$ must be treated separately. Then τ tends to a finite value τ_0 corresponding to a double Kelvin wave. τ_0 is found in terms of the solution to the cubic equation (8.21). The rate of change of τ with W is given by (8.31). When h is given by (9.1), the right-hand side of (8.33) reduces to

$$\frac{\beta}{1-\beta^2}\log\frac{1+\beta}{1-\beta} = 2\beta^2+\tfrac{8}{3}\beta^4+\ldots. \tag{9.27}$$

In particular when $\beta = \frac{1}{3}$ the above expression has the value 0·259,930. So from 8.23) and (8.33) we find

$$\tau_0 \sim 4{\cdot}496{,}48+6{\cdot}857{,}16W. \tag{9.28}$$

The first term in (9.28) is indicated by the horizontal line ($\tau = \tau_0$) in figure 5. However, the complete expression (9.28) lies so close to the numerically computed solution (see below) that it is indistinguishable from it graphically.

(*iii*) *Numerical solutions*

To evaluate ζ and τ over the range of W intermediate between 0 and ∞ a numerical integration of (6.2) was carried out. The procedure adopted was as follows. The parameter W was given. For some trial value of τ the pair of functions ζ and

$h\zeta'$ were integrated step by step from some large negative value of ξ (say $\xi = -10$) where ζ is exponential, up to $\xi = 0$. The values at $\xi = 0$ may be denoted by ζ_- and $h\zeta'_-$. A similar integration was carried out from $\xi = +10$ to $\xi = 0$, giving say ζ_+ and $h\zeta'_+$. Then the Wronskian

$$Z = h(\zeta_-\zeta'_+ - \zeta'_-\zeta_+) \tag{9.29}$$

was calculated. By repeating the process, Z was found as a function of τ. As expected, Z was an oscillatory function of τ. The roots of $Z = 0$, found by interpolation and successive approximation, gave the eigenvalues of the equation.

The values of τ computed in this way† are shown in figure 5 (full lines) plotted against the width W of the transition zone, in the case $\beta = \frac{1}{3}, \epsilon = 1$. It can be seen that the asymptotic behaviour of τ is verified at both large and small values of W. Thus τ tends to infinity at both ends of the range for all the modes except the lowest. For this last mode τ tends to a finite value as $W \to 0$, the value corresponding to a double Kelvin wave.

The corresponding eigenfunctions when $W = 8$, 1 and $\frac{1}{8}$ are shown in figures 6(*a*), (*b*) and (*c*) respectively. The functions have been normalized so that the integral of ζ^2 over $(-\infty < x < \infty)$ is equal to unity. The tendency for the lowest mode ($n = 0$) to be shifted towards the upper part of the transition zone can be seen in all three cases. In the higher modes this tendency is less apparent.

The reason for the near coincidence of the period of the lowest mode ($n = 0$) with the two asymptotes as $W \to 0$ and $W \to \infty$ may be worth investigating. Both asymptotes (9.14) and (9.28) represent straight lines (on a linear scale of W versus τ), and for the lowest mode ($\nu = 0$) both the gradient of the lines and their intercepts on the τ-axis are close together. The exact curve appears to lie between the two asymptotes.

Now for small values of β it is easy to show that the asymptote (8.34) reduces to

$$\tau \sim \frac{(1+\epsilon)^{\frac{1}{2}}}{\beta} + \frac{(1+\epsilon)}{\beta} W \quad \text{as} \quad W \to 0 \tag{9.30}$$

and the asymptote (9.10) reduces to

$$\tau \sim \frac{1+\epsilon}{\beta} W + (2\nu+1)\frac{(1+\epsilon)^{\frac{1}{2}}}{\beta} \quad \text{as} \quad W \to \infty. \tag{9.31}$$

(The proof of these results is left as an exercise to the reader.) For the lowest mode, the two above expressions are identical. The near coincidence of the asymptotes then appears as a result of the rather small value of β, $= \frac{1}{3}$, that we have selected.

In other words, the asymptotes will coincide if the contrast in depth between h_1 and h_2 is sufficiently small.

This, however, is a special property of the particular profile (9.1), as is evident from the fact that the asymptote for $W \to \infty$ generally depends on the *differential* properties of the depth profile at the point $\xi = \xi_0$ (§7, equation (7.23)) whereas

† The curves are based on the values of τ computed at the points $W = \frac{1}{8}$, $1/4\surd 2$, $\frac{1}{4}$, $1/2\surd 2$, ..., 8.

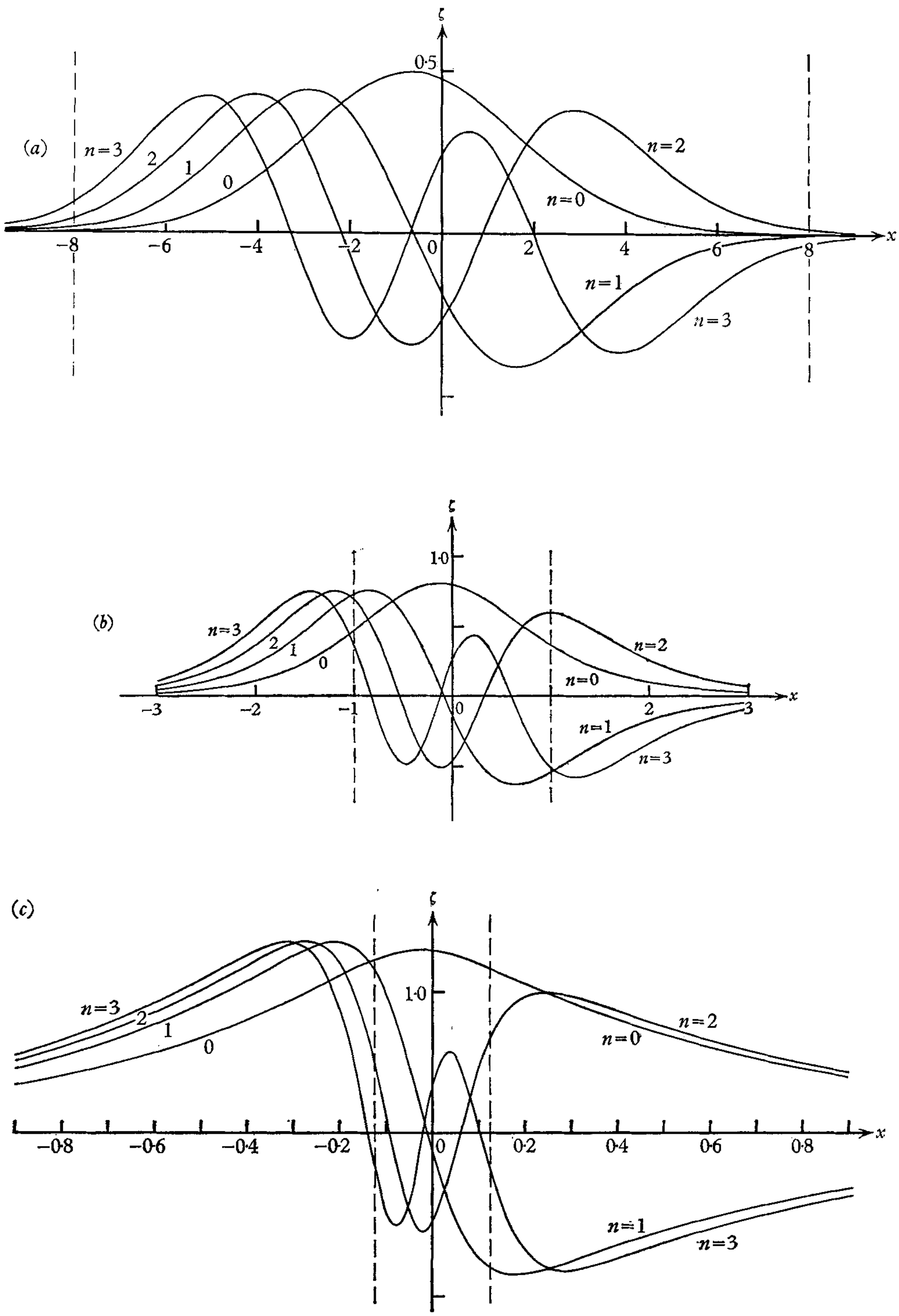

FIGURE 6. Eigenfunctions corresponding to the depth profile (1.1) when $\beta = \frac{1}{3}$ and $\epsilon = 1$. (*a*) $W = 8$, (*b*) $W = 1$, (*c*) $W = \frac{1}{8}$.

the asymptote for $W \to 0$ depends on an *integral* property of the depth (§8, equation (8.31)). A counter-example of a depth profile where the asymptotes do not coincide for small depth contrast will be given in the following section.

10. The 'uniform slope' profile

For the sake of comparison a similar study was carried out for the 'uniform slope' profile:

$$h/\bar{h} = \begin{cases} 1-\beta & (-\infty < \xi < -1), \\ 1+\beta\xi & (-1 < \xi < 1), \\ 1+\beta & (1 < \xi < \infty). \end{cases} \tag{10.1}$$

The corresponding analytical results are as follows:

(*i*) *Asymptotic behaviour as* $W \to \infty$

When $-1 < \xi < 1$ we have now

$$F = \bar{h}\beta(\epsilon' + \xi) \tag{10.2}$$

where ϵ' is given by (9.3). Thus

$$G(\xi, \lambda) = F - \lambda F' = \bar{h}\beta(\epsilon' + \xi - \lambda). \tag{10.3}$$

Clearly

$$\xi_0 = -1, \qquad \lambda_0 = \epsilon' - 1 \tag{10.4}$$

and

$$h_0 = \bar{h}(1-\beta), \qquad F_0 = \bar{h}\beta(\epsilon' - 1), \qquad F'_{0+} = \bar{h}\beta, \quad F''_{0+} = 0. \tag{10.5}$$

So the asymptotic form of ζ from (7.29) is given by

$$\zeta \sim Ai(\eta), \qquad \eta = \left(\frac{\beta}{1-\beta}\right)^{\frac{1}{3}} W^{\frac{2}{3}}(\xi + 1) + \eta_\nu \tag{10.6}$$

with

$$\tau \sim (\epsilon' - 1) W - \left(\frac{1-\beta}{\beta}\right)^{\frac{1}{3}} \eta_\nu W^{\frac{1}{3}}, \tag{10.7}$$

where η_ν denotes the νth zero of $Ai(\eta)$. For example, when $\beta = \frac{1}{3}$ and $\epsilon = 1$ we have

$$\tau \sim 6W - \sqrt{6}\,\eta_\nu W^{\frac{1}{3}}. \tag{10.8}$$

These asymptotes are indicated by the broken lines on the right of figure 7. The asymptote for the lowest mode ($\nu = 0$) is close to, but distinguishable from, the accurately calculated curve.

(*ii*) *Asymptotic behaviour as* $W \to 0$

For the higher modes we have, from (8.5), to solve

$$\frac{d}{d\xi}\left[(1+\beta)\frac{d\zeta}{d\xi}\right] + \bar{\lambda}\beta\zeta = 0 \qquad (\bar{\lambda} = W\tau), \tag{10.9}$$

with boundary conditions

$$d\zeta/d\xi = 0 \quad \text{when} \quad \xi = \pm 1. \tag{10.10}$$

The change of variable

$$\rho = 2(1 + \beta\xi)^{\frac{1}{2}} \tag{10.11}$$

reduces equation (10.9) to Bessel's equation

$$\frac{d^2\zeta}{d\rho^2}+\frac{1}{\rho}\frac{d\zeta}{d\rho}+\frac{\bar{\lambda}}{\beta}\zeta = 0 \tag{10.12}$$

with boundary conditions

$$d\zeta/d\rho = 0 \quad \text{when} \quad \rho = 2(1\pm\beta)^{\frac{1}{2}}. \tag{10.13}$$

The solution is then $\zeta = AJ_0[\rho(\bar{\lambda}/\beta)^{\frac{1}{2}}]+BY_0[\rho(\bar{\lambda}/\beta)^{\frac{1}{2}}]$. (10.14)

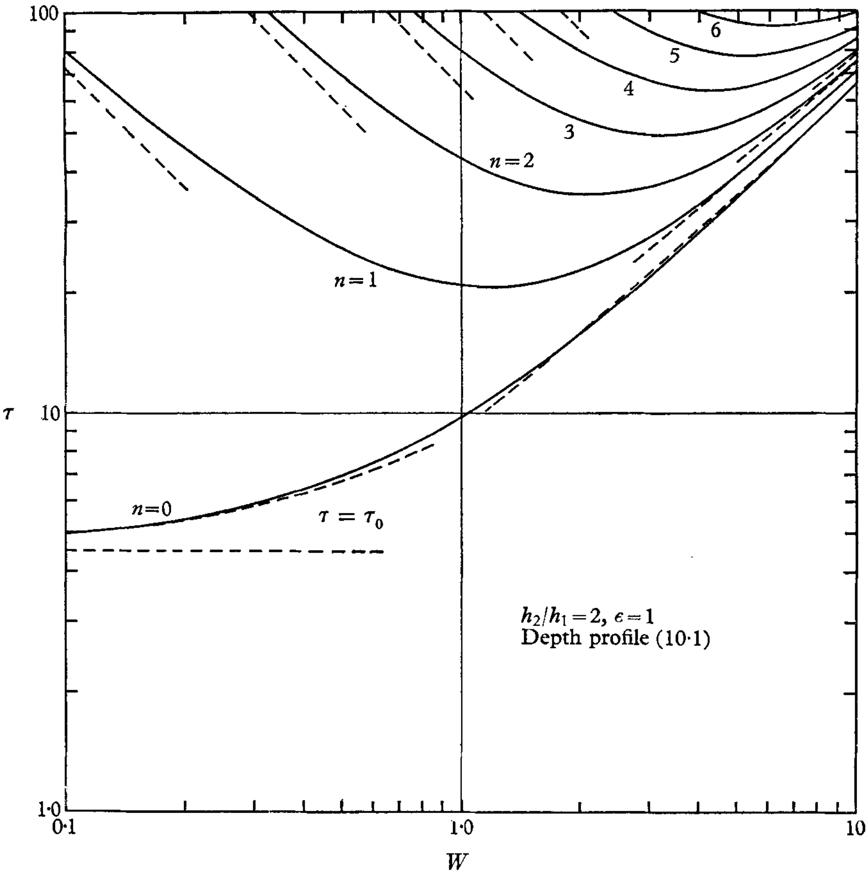

FIGURE 7. The wave period as a function of the width W of the transition zone for the 'uniform slope' profile (10.1), with $\beta = \frac{1}{3}$, $\epsilon = 1$. Full curves represent the computed values, broken curves the asymptotes.

Since $J_0' = -J_1$ the boundary conditions give

$$\left.\begin{aligned} AJ_1(a)+BY_1(a) &= 0, \quad a = 2[\bar{\lambda}(\beta^{-1}-1)]^{\frac{1}{2}}, \\ AJ_1(b)+BY_1(b) &= 0, \quad b = 2[\bar{\lambda}(\beta^{-1}+1)]^{\frac{1}{2}}. \end{aligned}\right\} \tag{10.15}$$

Hence $U(a,b) \equiv J_1(a)Y_1(b)-J_1(b)Y_1(a) = 0$ (10.16)

and $a/b = \left(\frac{1-\beta}{1+\beta}\right)^{\frac{1}{2}} = \left(\frac{h_1}{h_2}\right)^{\frac{1}{2}}.$ (10.17)

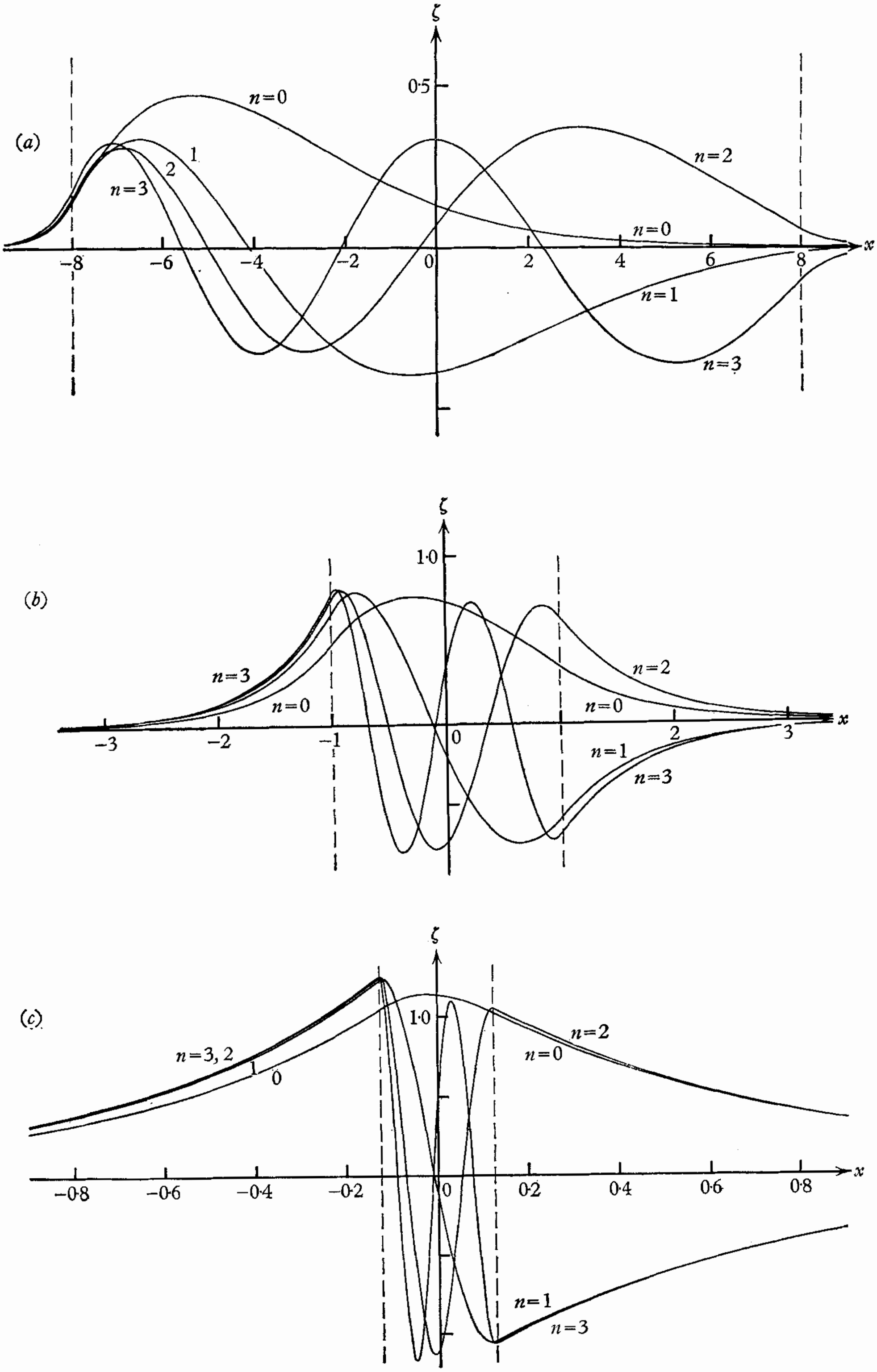

FIGURE 8. Eigenfunctions corresponding to the 'uniform slope' (1.2) when $\beta = \frac{1}{8}$ and $\epsilon = 1$. (*a*) $W = 8$, (*b*) $W = 1$, (*c*) $W = \frac{1}{8}$.

The curves in the (a, b)-plane corresponding to $U = 0$ are shown in figure 9. They are easily plotted, for if z_s denotes the sth zero of $J_1(z)$, then the sth curve passes through the points $(a, b) = (z_s, z_{s+n})$ indicated by solid circles. Similarly with the zeros of $Y_1(z)$ (indicated by empty circles). Moreover, zeros of $U(a, b)$ for given ratios a/b have been tabulated by various authors, for example, by Fox (1950) and Olver (1964). To find the values of (a, b) for a given value of β

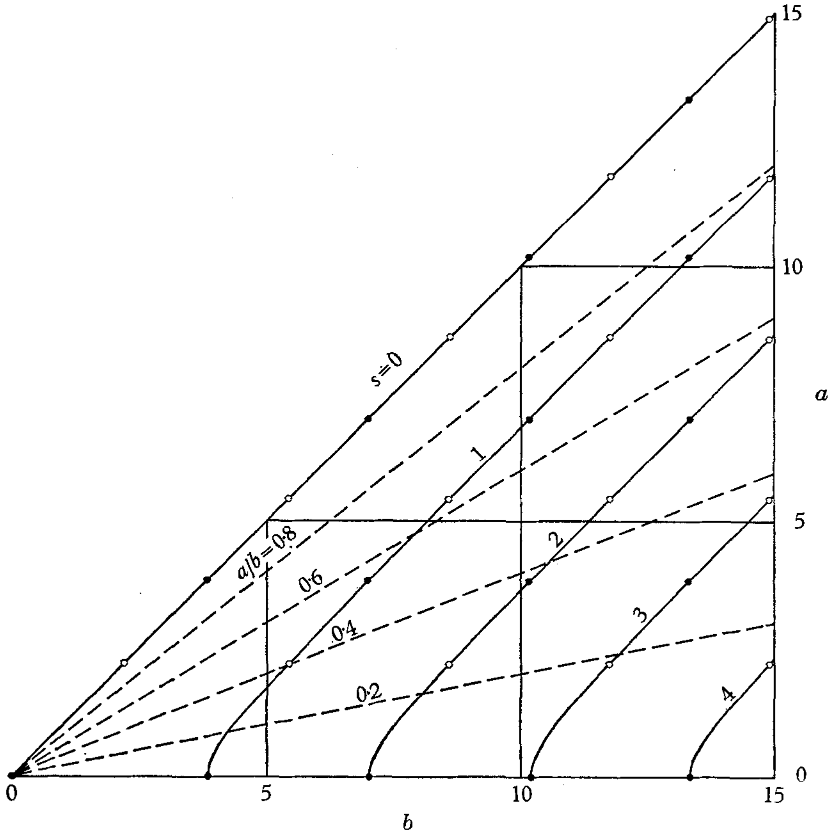

FIGURE 9. Diagram for the solution of the equation $U(a, b) \equiv J_1(a)\,Y_1(b) - J_1(b)\,Y_1(a) = 0$. Full curves represent the zero-contours of U. Full circles indicate points with co-ordinates (z_s, z_{n+s}) where z_s is a zero of $J_1(z)$. Open circles indicate points (z'_s, z'_{n+s}) where z'_s is a zero of $Y_1(z)$.

we may take the intersections of the straight line (10.17) with the curves of figure 9. Each intersection gives a pair (a_n, b_n), say. Then from (10.15) we have

$$\bar{\lambda} = \bar{\lambda}_n = \frac{\beta}{1-\beta^2}\frac{a_n b_n}{4}. \tag{10.18}$$

For example, in the case $\beta = \frac{1}{3}$ we find the values of $\bar{\lambda}$ shown in the last column of table 1. These may be compared with the corresponding values for the profile (9.1), which are shown in column 2 of the same table. It will be seen that for the higher modes the wave periods for the bottom profile (10.1) are almost twice as great as those for the profile (9.1). However, for the lowest mode ($n = 0$) both a_n and b_n vanish, and τ tends to the same finite value which corresponds to the double Kelvin wave. The expression on the right of (8.33) reduces to

$$\frac{2}{1-\beta^2}-\frac{1}{\beta}\log\frac{1+\beta}{1-\beta} = \tfrac{4}{3}\beta^2+\tfrac{8}{5}\beta^4+\dots. \tag{10.19}$$

The first term of the asymptote (8.34), namely $\tau \sim \tau_0$, is indicated by the broken horizontal line in figure 7. (This is the same as in figure 5.) The complete expression in (8.34) is indicated by the lowest broken curve to the left of figure 7. This again is close to, but easily distinguishable from, the accurately computed curve. We may note that for small values of β the asymptote (8.34) reduces to

$$\tau \sim \frac{(1+\epsilon)^{\frac{1}{2}}}{\beta}+\frac{2}{3}\frac{(1+\epsilon)}{\beta}W \quad \text{as} \quad W\to 0, \tag{10.20}$$

while (10.7) reduces to

$$\tau \sim \frac{1+\epsilon}{\beta}W-\frac{\eta_\nu}{\beta^{\frac{1}{3}}}W^{\frac{1}{3}} \quad \text{as} \quad W\to\infty. \tag{10.21}$$

These are clearly not the same (cf. §9).

The accurately computed periods for the normal modes are shown by the full curves in figure 7, and the corresponding eigenfunctions are shown in figure 8 for $W = 8$, 1 and $\frac{1}{8}$. These figures may be compared to figures 5 and 6 respectively. The behaviour of the modes in figure 8 is similar to that in figure 6. In figure 8 there is a similar tendency for the energy to be shifted towards the left, that is to say the upper part of the slope. The tendency is most pronounced in the lowest mode in figure 8*a*.

11. The dispersion relation

In §§7–10 we have discussed the behaviour of the wave period τ, and hence the frequency $\sigma = -1/\tau$, for a fixed wave-length in the y-direction and varying horizontal scales in the x-direction. Of equal importance, however, is the dependence of the frequency σ on the wave-number m in the y-direction, when the bottom profile is kept constant. The derivative $d\sigma/dm$ gives in fact the group-velocity of the waves.

It might at first be thought that the bottom profile would appear to a longer wave as a very steep slope, that is to say that limiting behaviour as $m\to 0$ or $m\to\infty$ would be similar to the behaviour as $W\to 0$ or $W\to\infty$ respectively. Although this is true in the non-divergent approximation, there are, as we shall see, important differences between the limiting cases as $m\to\infty$ and $W\to\infty$, due to the divergence of the wave motion.

When the wave-number m is retained in the differential equation (2.6), but f is set equal to unity, we obtain

$$(h\zeta')' = \left(\frac{\tau^2-1}{g\tau^2}+m^2h-m\tau h'\right)\zeta. \tag{11.1}$$

Consider first the limit as $m \to \infty$. Setting

$$\tau/m = \lambda = O(1) \tag{11.2}$$

we see that (11.1) can be written

$$(h\zeta')' = m^2(F - \lambda F')\zeta, \tag{11.3}$$

where
$$F = h + \frac{\lambda^2 m^2 - 1}{g\lambda^2 m^4} = h + O(m^{-2}). \tag{11.4}$$

Comparing this with (7.1) and (7.2) we see that the situations are similar except that W is replaced by m, and $F \sim h + (1/g)$ is replaced by $F \sim h$. So in *this* limiting case the divergence may be neglected. The asymptotic formulae for ζ and τ may be written down directly from § 7. For example, from (7.23) we have in the case of the smooth profile

$$\sigma \sim -\frac{h'_{0+}}{h_0} m^{-1} + (2\nu + 1)\left[\frac{h'_0(h'_0 h''_0 - h_0 h'''_0)}{2h_0^3}\right]^{\frac{1}{2}} m^{-2}, \tag{11.5}$$

where h_0 is the solution of
$$(\log h_0)'' = 0. \tag{11.6}$$

In the case when h is continuous but h' discontinuous we have

$$\sigma \sim -\frac{h'_0}{h_0} m^{-1} + \eta_\nu \left[\frac{h'^2_{0+} - h_0 h''_{0+}}{h_0^3}\right]^{\frac{1}{3}} m^{-\frac{5}{3}}, \tag{11.7}$$

where η_ν is a zero of the Airy function and h_0 is the depth at the discontinuity.

Consider on the other hand the limit $m \to 0$. On writing equation (11.1) as

$$(h\zeta')' = \left(m^2 h + \frac{\bar{\lambda}^2 - m^2}{g\bar{\lambda}^2} - \bar{\lambda} h'\right)\zeta, \tag{11.8}$$

where
$$\bar{\lambda} = m\tau = O(1), \tag{11.9}$$

we see that as $m \to 0$ the limiting form of this equation is now

$$(h\zeta')' = \left(\frac{1}{g} - \bar{\lambda} h'\right)\zeta \tag{11.10}$$

with boundary conditions that $\zeta \to 0$ as $x \to \pm\infty$. A discrete set of eigenvalues $\bar{\lambda} = \bar{\lambda}_n$, where $n = 0, 1, 2, \ldots$ will, in general, exist, as that as $m \to 0$,

$$\sigma \sim -m/\bar{\lambda}_n. \tag{11.11}$$

But in contrast to (8.5), equation (11.10) has no eigenvalue $\bar{\lambda} = 0$. Since the coefficient of ζ must be negative over at least some range of x we must have

$$\bar{\lambda} > \frac{1}{(gh')_{\max}} > 0. \tag{11.12}$$

So there exists no mode whose period and frequencies tend to finite non-zero limits as $m \to 0$.

The difference between this situation and the limit as $W \to 0$ is connected with the presence of the term $1/g$ on the right of (11.10); which again is associated with the divergence of the wave motion. Since m occurs in the denominator of the parameter ϵ (see (4.21)) the divergence is of course most pronounced at small values of m, corresponding to large wavelengths.

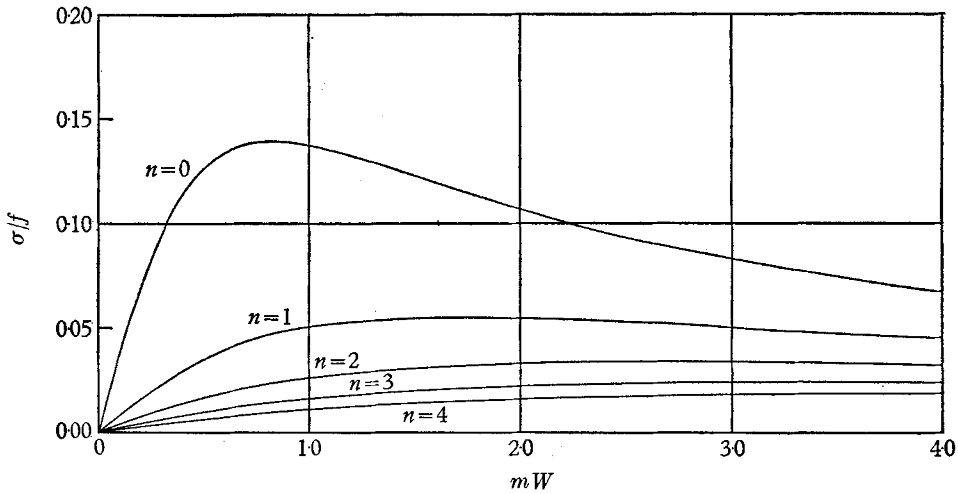

FIGURE 10. Dispersion relation showing the frequency σ/f as a function of mW when $h_2/h_1 = 2$ ($\beta = \frac{1}{3}$) and the convergence parameter $\varpi = 1$.

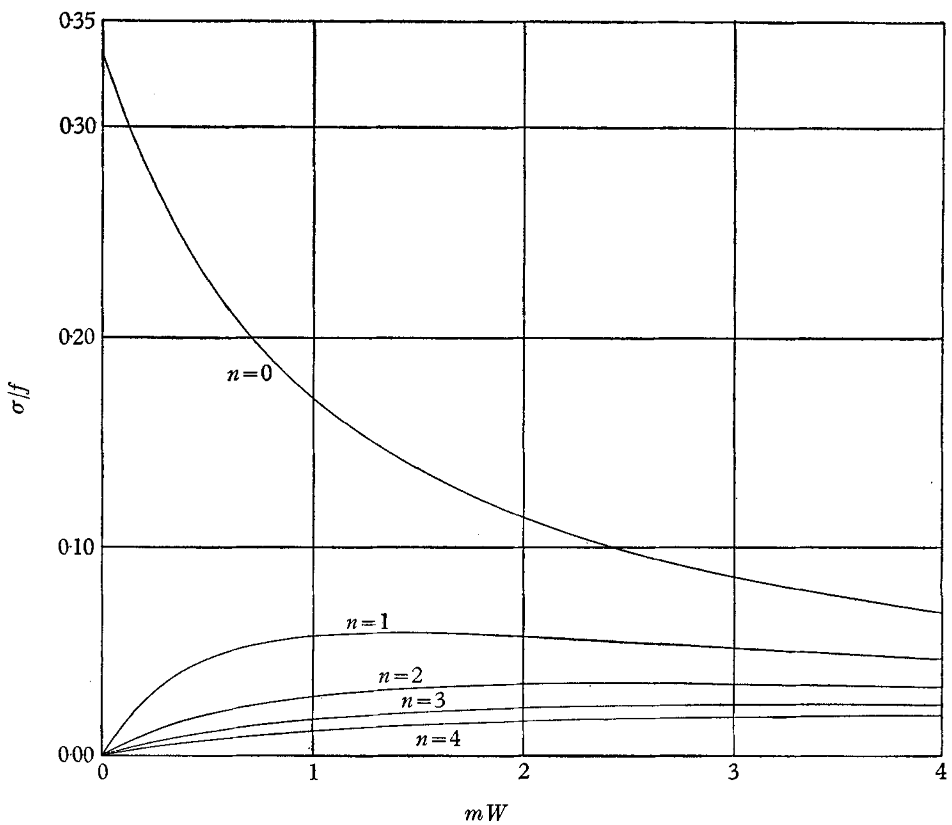

FIGURE 11. As in figure 10, but with $\varpi = 0$ (non-divergent waves).

A consequence of (11.11) and (11.12) is that for large wavelengths the phase velocity tends to a finite limiting value:

$$c = -\sigma/m \to 1/\overline{\lambda}_n < f(gh')_{\max} \tag{11.13}$$

(the formula has been made dimensional by inserting the Coriolis frequency f.) At small wavelengths (large m) equations (11.5) and (11.7) show that the phase velocity c tends to zero.

From (11.13) it follows also that the group velocity at large wavelengths is in the same direction, and in fact is equal to the phase velocity; while from (11.5) and (11.7) the group velocity is in the opposite direction to the phase velocity. Thus if the group velocity is continuous it must vanish somewhere in the interval $0 < m < \infty$.

The dispersion relation for the smooth profile (9.1) was computed for two values of the parameter

$$\varpi \equiv \frac{Wf^2}{(gh')_{\max}} = \frac{W^2f^2}{\beta g\bar{h}}, \tag{11.14}$$

namely $\varpi = 1$ (figure 10) and $\varpi = 0$ (figure 11). As before, $\beta = \frac{1}{3}$. The scale is now linear in σ and m. The marked difference in the behaviour of the lowest mode can be seen, especially on the left of the diagram. The effect on the higher modes is less pronounced. In general, the effect of taking the divergence into account is to shift the maximum value of each curve towards the right. In other words the wave-number associated with vanishing group-velocity tends to be increased.

12. Discussion

We have investigated in detail only two special forms of the depth profile $h(x)$. But from the asymptotic formulae given in §§7, 8 and 11 it should be possible to construct by elementary means a rough approximation to the wave period τ as a function of m for any given form of h or value of ϖ. It appears likely that, at least for small values of W, the form of the lowest mode is insensitive to the details of the bottom topography, and differs little from a double Kelvin wave. The higher modes, to judge by their wave periods, are more sensitive to the bottom topography, and so might be more easily scattered by irregularities in the bottom profile.

In the present treatment we have made various simplifying assumptions, in particular that the depth profile is monotonic, and that the gradient is reasonably smooth. If the profile is monotonic but not smooth, then the function Q in (3.14), which depends on the derivative of h with respect to x, will be spiky. Under such circumstances we expect that those modes whose scale in the x-direction is large compared to the horizontal scale of the bottom roughnesses will not be much affected, but that those whose scale is comparable with, or small compared to the roughnesses will be quite different.

If $h(x)$ is not even monotonic then the way is open for modes which travel in the opposite direction to Kelvin waves, that is, modes having $\tau < 0$. Trapped waves with period less than a pendulum-day also become possible. Among these may be included waves which are refracted towards the shallower part of the transition zone by the ordinary process of wave refraction (see, for example, Eckart 1951; Longuet-Higgins 1967).

It would be interesting to observe the pattern of currents near some prominent feature in the ocean such as the Mendocino escarpment in the Pacific, to see if oscillations corresponding to double Kelvin waves do in fact exist. For reasons given in paper I, one might expect to find a high density of energy in the neighbourhood of the cut-off period, corresponding to high wave-numbers and zero divergence. This is given by

$$\tau = \frac{h_2+h_1}{h_2-h_1} \tag{12.1}$$

in units of a pendulum-day. To detect such oscillations by harmonic analysis it would be desirable to make continuous observations over a period of at least several weeks.

The present investigation was begun at the National Institute of Oceanography, England in the summer of 1967. The computations reported in §§8 and 9 were for the most part carried out on the Atlas computer at London University with the assistance of Mr H. Griffiths, of N.I.O. They were completed by the author on the CDC 3300 at Corvallis. The work at Corvallis has been supported under ONR Contract 30-4544. The author would like to acknowledge the stimulus of conversations with Dr K. Hasselmann on a visit to Hamburg University and of correspondence with Dr V. T. Buchwald at the University of Sydney.

REFERENCES

Antosiewicz, H. A. 1964 Bessel functions of fractional order. Chapter 10, pp. 435–478 in *Handbook of Mathematical Functions*, U.S. Nat. Bur. Standards Appl. Math. Ser. 55, Washington, D. C. 1046 pp.

Buchwald, V. T. & Adams, J. K. 1968 The propagation of continental shelf waves. *Proc. Roy. Soc.* A, in press.

Eckart, C. 1951 Surface waves on water of variable depth. *U.S. Office of Naval Research. Wave Rept.* no. 100. (Notes of lectures given at the Scripps Institution of Oceanography.)

Fox, L. 1950 *Brit. Ass. Math. Tables*, vol. **6**: *Bessel Functions. Pt. I. Functions of orders zero and unity.* Cambridge University Press.

Longuet–Higgins, M. S. 1965 Some dynamical aspects of ocean currents. *Quart. J. Roy. Meteor. Soc.* **91**, 425–457.

Longuet-Higgins, M. S. 1967 On the trapping of wave energy round islands. *J. Fluid Mech.* **29**, 781–821.

Longuet-Higgins, M. S. 1968 On the trapping of waves along a discontinuity of depth in a rotating ocean. *J. Fluid Mech.* **31**, 417.

Miller, J. C. P. 1946 *The Airy integral. Brit. Ass. Adv. Sci. Mathematical Tables Part*— vol. **B**. Cambridge University Press.

Olver, F. W. J. 1955 The asymptotic solution of linear differential equations of the second order for large values of a parameter. *Phil. Trans.* A **247**, 307–327.

Olver, F. W. J. 1964 Bessel functions of integer order. Chapter 9, pp. 355–434 in *Handbook of Mathematical Functions*, U.S. Nat. Bur. Standards Appl. Math. Ser. 55. Washington, D.C. 1046 pp.

Phillips, N. A. 1965 Elementary Rossby waves. *Tellus*, **17**, 295–301.

Rhines, P. B. 1967 *The influence of bottom topography on long-period waves in the ocean.* Ph.D. dissertation, Cambridge University.

Shinbrot, M. 1963 Note on a nonlinear eigenvalue problem. *Proc. Am. Math. Soc.* **14**, 552–558.